Mössbauer and EPR Studies of the Photoactivation of Nitrile Hydratase†

Victoria-Codrina Popescu,‡,|| Eckard Münck,‡ Brian G. Fox,‡,⊥ Yiannis Sanakis,‡,@ John G. Cummings,§ Ivan M. Turner, Jr.,§ and Mark J. Nelson*,§

Department of Chemistry, Carnegie Mellon University, Pittsburgh, Pennsylvania 15213, and Central Research and Development, DuPont, Wilmington, Delaware 19880-0328

Received January 31, 2001; Revised Manuscript Received May 10, 2001

ABSTRACT: The $\alpha\beta$ dimer of active nitrile hydratase from *Rhodococcus* sp. R312 contains one low-spin ferric ion that is coordinated by three Cys residues, two N-amide groups from the protein backbone, and one OH^-. The enzyme isolated from bacteria grown in the dark is inactive and contains the iron site as a six-coordinate diamagnetic Fe−nitrosyl complex, called NH_{dark}. The active state can be obtained from the dark state by photolysis of the Fe−NO bond at room temperature. Activation is accompanied by the conversion of NH_{dark} to a low-spin ferric complex, NH_{light}, exhibiting an $S = {}^1/_2$ EPR signal with g values of 2.27, 2.13, and 1.97. We have characterized both NH_{dark} and NH_{light} with Mössbauer spectroscopy. The z-axis of the ^{57}Fe magnetic hyperfine tensor, **A**, of NH_{light} was found to be rotated by ∼45° relative to the z-axis of the **g** tensor ($g_z = 1.97$). Comparison of the **A** tensor of NH_{light} with the **A** tensors of low-spin ferric hemes indicates a substantially larger degree of covalency for nitrile hydratase. We have also performed photolysis experiments between 2 and 20 K and characterized the photolyzed products by EPR and Mössbauer spectroscopy. Photolysis at 4.2 K in the Mössbauer spectrometer yielded a five-coordinate low-spin ferric species, NH_A, which converted back into NH_{dark} when the sample was briefly warmed to 77 K. We also describe preliminary EPR photolysis studies that have yielded new intermediates.

Nitrile hydratases are bacterial metalloenzymes that catalyze the hydration of nitriles to amides (*1*). Members of a subclass of these enzymes contain iron and are present in an inactive form in cells grown in the dark (*2*). Purification in the dark leads to a purified inactive enzyme (NH_{dark})[1] (*3*). Exposure of NH_{dark} to near-UV light at room temperature results in the production of an active enzyme (NH_{light}) (*4*). It has been shown that NH_{dark} contains a diamagnetic iron−nitrosyl complex and that the NO ligand dissociates from the active site of the enzyme in the process of activation (*5*−*8*). Treatment of NH_{light} with nitric oxide in the dark results in regeneration of NH_{dark}, which then can be reactivated by exposure to light (*7*, *8*). This reversible conversion has been suggested to be a regulatory mechanism for nitrile hydratase in its environment, but supporting evidence for such biological relevance is lacking. NH_{light} is metastable, but catalytic activity can be maintained in the presence of butyric acid, a competitive inhibitor that significantly alters the spectroscopic properties of the iron (*9*).

The active form of the iron-containing nitrile hydratases contains a low-spin ($S = {}^1/_2$) ferric complex in an unusual N, S, O coordination environment that has been characterized extensively by EPR, ENDOR, resonance Raman, and EXAFS spectroscopies (*10*−*15*). The 2.65 Å crystal structure of NH_{light} from *Rhodococcus* sp. R312 shows three cysteine thiolate ligands in a *facial* orientation and two peptide amide N-donor ligands; the sixth coordination site appeared to be vacant (*16*). However, ENDOR spectroscopy on frozen solution samples provides evidence for the coordination of a hydroxide ligand in the sixth coordination site of the Fe^{3+} in NH_{light} samples containing butyric acid (*13*). A 1.7 Å crystal structure of NH_{dark} is consistent with a nitrosyl ligand in the sixth coordination site of the iron in that state (Figure 1) and suggests that the three cysteine ligands occur in different oxidation states, namely, as a thiolate (Cys109), as a sulfinic acid (−SOH, Cys112), and as a sulfenic acid [−S(O)OH, Cys114] (*17*).

The resonance Raman spectra of NH_{dark} are similar to those of NH_{light} in the low-energy, metal−ligand stretching region (*6*, *14*). For the latter, it has been demonstrated that the Raman spectra arise in large part from coupling between Fe−S stretches and the side chain vibrations of the associated cysteine residues. Thus, it appears that the sulfur ligands coordinated at the iron maintain their oxidation state throughout the photoactivation−inactivation process. In the simplest model for the mechanism of activation of nitrile

† Supported by NIH Grant 22701 (E.M.).

* To whom correspondence should be addressed. Phone: (302) 695-4124. Fax: (302) 695-4260. E-mail: Mark.J.Nelson@usa.dupont.com.

‡ Carnegie Mellon University.

§ DuPont.

|| Current address: Department of Biochemistry, Molecular Biology and Biophysics, University of Minnesota, Minneapolis, MN 55455.

⊥ Current address: Department of Biochemistry, University of Wisconsin, Madison, WI 53705.

@ Current address: Institute of Materials Science, NCRR "Demokritos", Attiki, Greece.

[1] Abbreviations: NH_{dark}, inactive form of nitrile hydratase obtained by cell growth and enzyme purification in the dark; NH_{light}, enzymatically active form of nitrile hydratase obtained by illumination of NH_{dark}; NH_C, paramagnetic species obtained by illumination of NH_{dark} at 2−5 K in EPR experiments; NH_A and NH_B, paramagnetic species obtained by illumination of NH_{dark} in Mössbauer experiments at 4.2 and 150−180 K, respectively; HEPES, *N*-(2-hydroxyethyl)piperazine-*N*-2-ethanesulfonic acid.

10.1021/bi010198f CCC: $20.00
Published on Web 06/12/2001

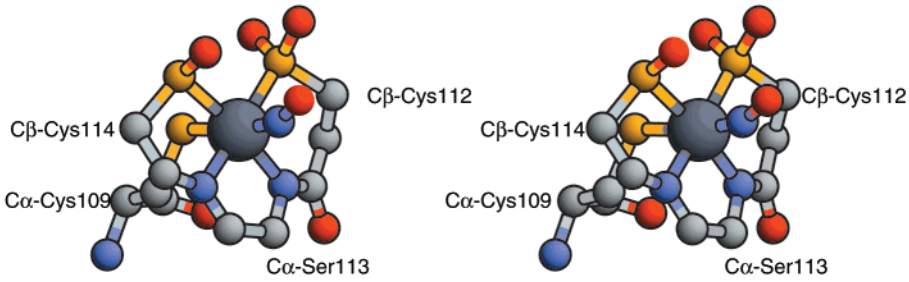

FIGURE 1: Divergent stereoview of the structure of the iron site in NH_{dark} prepared from Protein Data Bank entry 2AHJ. Amino acids providing iron ligands are as indicated. NO occupies an axial coordination position opposite of S_γ from Cys109. Atom colors are as follows: light gray, carbon; blue, nitrogen; red, oxygen; yellow, sulfur; dark gray, iron.

hydratase, the difference between the iron complexes in NH_{light} and NH_{dark}, consistent with the crystal structures and the spectroscopic data, is that a hydroxide ligand in NH_{light} is substituted for a nitrosyl ligand in NH_{dark}. The inactivity of NH_{dark}, then, supports the notion that either the nitrile substrate binds to the iron at the sixth coordination position by substitution of the OH^- ligand or the coordinated hydroxide is a reactant in the catalytic nitrile hydration (*16*).

The mechanism of the photoactivation reaction in nitrile hydratase has been the subject of several spectroscopic investigations. Originally, it was suggested that photoactivation involved electron transfer from a mixed-valence diiron cluster to an electron acceptor on the protein (*4*, *18*). This was an attempt to reconcile Mössbauer spectroscopic data showing a mixture of ferrous and ferric iron in NH_{dark} with magnetic susceptibility data showing that this state was diamagnetic. The presence of a binuclear cluster is in conflict with both of the crystal structures that are now available for the protein (*16*, *17*). More recently, FTIR and resonance Raman studies suggested that photoactivation involves photolysis of nitric oxide from a diamagnetic $Fe^{3+}-NO$ complex (*5*, *6*). This, however, is difficult to reconcile with the published Mössbauer data. To resolve that discrepancy, we have studied nitrile hydratase in both the NH_{dark} and NH_{light} states with Mössbauer spectroscopy. We have also illuminated NH_{dark} at cryogenic temperatures and obtained evidence for additional states of the enzyme that form under these conditions. We suggest that these states may be intermediates in the photoactivation process, with one (NH_A) representing a state in which the Fe−NO bond is broken but the NO is still "caged" in the vicinity of the active site. Our Mössbauer and preliminary EPR spectra suggest that these additional states are different from the previously characterized active form of nitrile hydratase, NH_{light}, and that most or all are five-coordinate complexes obtained by photolyzing the Fe−NO bond. These complexes exhibit EPR and Mössbauer properties typical for low-spin ferric sites, which are rarely observed for five-coordinate ferric complexes.

MATERIALS AND METHODS

Nitrile Hydratase Purification. NH_{dark} was purified from *Rhodococcus* sp. R312 cells grown in the dark (*19*) and assayed as described previously (*14*). Unless stated otherwise, samples of NH_{light} were prepared by exposing samples of NH_{dark} on ice to ambient light for 30−60 min. Aliquots were taken for assay, and the activation was deemed complete when there was no further increase in enzyme activity. Protein samples were prepared in 0.1 M *N*-(2-hydroxyethyl)-piperazine-*N*-2-ethanesulfonic acid (HEPES) with 0.04 M sodium butyrate adjusted to pH 7.0 (at room temperature), and were diluted into glycerol for particular experiments as stated.

EPR Spectroscopy. EPR spectra of NH_{light} and NH_C were obtained as previously described (*14*). Samples of NH_C were generated at DuPont by exposing a sample of NH_{dark} in the EPR cryostat to broad-spectrum light generated by a Cermax LX300UV xenon illuminator with a total output of approximately 0.05 W/nm over the range from 300 to 800 nm. The light was filtered through 6 cm of circulating tap water to filter IR radiation. EPR illumination experiments were carried out at Carnegie-Mellon by illuminating for 30 min an EPR sample of NH_{dark} (200 μL, 0.2 mM) maintained at ≈2 K in the cavity of the spectrometer. The light from a projector lamp (150 W) was directed on the lateral opening of the cavity through a round-bottom flask filled with water (4 cm diameter, for filtering the IR radiation). All EPR spectra were analyzed using a software package written by M. P. Hendrich at Carnegie Mellon University.

Mössbauer Spectroscopy. Mössbauer spectra were recorded with constant acceleration spectrometers. The samples were inserted into Janis Research, Inc., helium dewars equipped with sensors that allow the temperature of the sample to be controlled from 4.2 to 200 K. One cryostat houses a superconducting magnet, and magnetic fields of up to 8.0 T can be applied parallel to the observed γ-radiation. For the second spectrometer, a magnetic field of 450 G was applied with a permanent magnet placed parallel or perpendicular to the observed γ-radiation. Isomer shifts are quoted relative to Fe metal at 298 K. Unless stated otherwise, protein samples were prepared by freezing the sample in liquid nitrogen in a plastic Mössbauer cuvette.

For the Mössbauer photolysis experiments, the buffered enzyme was mixed with glycerol (50:50 v/v, ^{57}Fe concentration ≈ 1 mM) and filled into a cylindrical Lucite cuvette (9 mm diameter × 6 mm). The cuvette was mounted in the tail section of a helium cryostat in a brass assembly at the end of a vertical suspension system. The brass assembly was equipped with heater wires and temperature sensors. The main part of the suspension system consisted of a 1 cm diameter Lucite rod 120 cm in length. This rod served both as a mechanical support for the brass assembly and as a pipe for guiding the light from a 300 W slide projector to the sample cuvette. The top of the rod, approximately 30 cm above the top flange of the cryostat, had a conical Lucite extension piece for light collection glued to the suspension rod by dissolving the surfaces with dichloroethane. A water-filled round-bottom flask (≈6 cm diameter) was placed

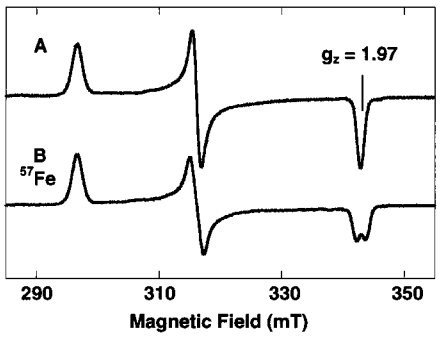

FIGURE 2: EPR spectra of NH_{light}. (A) Sample containing ^{57}Fe in natural abundance (2.2%). (B) Sample containing ^{57}Fe enriched to >90%. Experimental conditions: temperature, 40 K; microwave frequency, 9.46 GHz; modulation amplitude, 1 mT; microwave power, 2 mW.

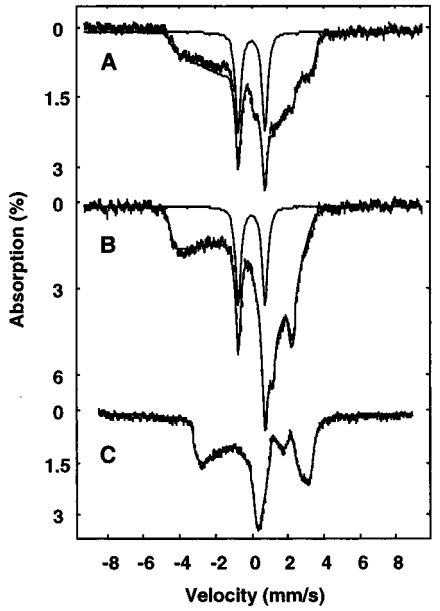

FIGURE 3: Mössbauer spectra of NH_{light} recorded at 4.2 K in 50 mT fields applied perpendicular (A) and parallel (B) to the incident γ-beam, and a parallel 8.0 T applied field (C). The quadrupole doublet outlined above the spectra belongs to NH_{dark}. The solid lines drawn through the spectra are theoretical curves representing the sum of two spectral components: a paramagnetic ($S = {}^1/_2$) component (NH_{light}; 84% of the total Fe) and the diamagnetic component of NH_{dark} (16% of the total Fe). The data in panel C were obtained by subtracting the contribution of NH_{dark} from the 8.0 T spectrum. The theoretical spectrum of NH_{light} was generated from eq 1 using the parameters listed in Table 1.

between the projector and the conical top of the Lucite light pipe for focusing and filtering of IR radiation.[2] The Mössbauer spectra were analyzed using the software package WMOSS (WEB Research, Edina, MN).

RESULTS

Mössbauer Study of NH_{light}. As reported previously (*10*), active nitrile hydratase contains a low-spin ($S = {}^1/_2$) ferric ion characterized by an EPR spectrum with the following g values: $g_x = 2.27$ $g_y = 2.13$, and $g_z = 1.97$ (Figure 2A). Figure 3 displays 4.2 K Mössbauer spectra of NH_{light} recorded

[2] This assembly was designed for studies of hydrogenase. Major ideas in the conception of this setup were contributed by S. Albracht of the University of Amsterdam (Amsterdam, The Netherlands), whose help is greatly appreciated.

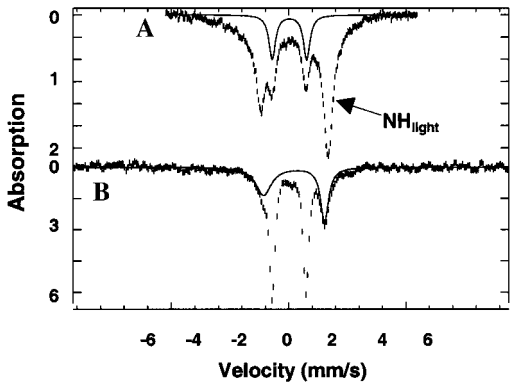

FIGURE 4: The 150 K Mössbauer spectra of NH_{light} (A) and NH_B (B). (A) The spectrum of NH_{light} (same sample as in Figure 3) was recorded at 150 K in a parallel magnetic field of 50 mT. The solid line indicates the contribution of NH_{dark}. (B) NH_{dark} was illuminated for 15 min at 150 K, and the spectrum was recorded for 20 h at this temperature. The quadrupole doublet attributed to NH_B is drawn above the data.

in a 0.05 T magnetic field applied perpendicular (Figure 3A) and parallel (Figure 3B) to the observed γ-radiation. The spectra reveal two distinct components. One component, accounting for 16% of the iron in the sample, contributes a sharp doublet with a quadrupole splitting, ΔE_Q, of 1.47 mm/s and an isomer shift, δ, of 0.03 mm/s. This species is diamagnetic and represents NH_{dark} (see below) resulting from incomplete photoactivation. The second component exhibits paramagnetic hyperfine structure and belongs to the low-spin ferric ion of NH_{light}. Figure 3C shows a 4.2 K Mössbauer spectrum recorded in an 8.0 T applied field; we have subtracted the contribution of the NH_{dark} (16%) from the raw data for clarity.

The observation of magnetic hyperfine structure in the spectrum of NH_{light} in parts A and B of Figure 3 implies that the electronic spin relaxation is slow ($<10^6$ s^{-1}) on the Mössbauer time scale. At 150 K, however, the electronic spin relaxes sufficiently fast that the magnetic hyperfine interactions are averaged out to a large extent (Figure 4). The two outermost lines in the spectrum of Figure 4A belong to NH_{light} ($\Delta E_Q \approx 2.8$ mm/s and $\delta \approx 0.25$ mm/s at 150 K). The quadrupole doublet seen in the 4.2 K spectrum of Figure 3 and assigned to NH_{dark} is also present in the high-temperature data and indicated by the solid line in Figure 4A.

We have analyzed the low-temperature spectra of NH_{light} (Figure 3) using the $S = {}^1/_2$ spin Hamiltonian

$$H = \beta \mathbf{S}\cdot\mathbf{g}\cdot\mathbf{B} + \mathbf{S}\cdot\mathbf{A}\cdot\mathbf{I} - g_n\beta_n\mathbf{B}\cdot\mathbf{I} + (eQV_{z'z'}/12)[3I_{z'}^2 - 15/4 + \eta(I_{x'}^2 - I_{y'}^2)] \quad (1)$$

where all quantities have their conventional meanings, $\eta = (V_{x'x'} - V_{y'y'})/V_{z'z'}$ is the asymmetry parameter of the electric field gradient (EFG) tensor, and the primed coordinates refer to the principal axis system of the EFG tensor (*20*). The solid lines drawn through the data of Figure 3 are theoretical curves generated from eq 1 using the parameters listed in Table 1. Our simulations show that the largest component of the electric field gradient ($V_{z'z'}$) is collinear with the largest component of the magnetic hyperfine tensor ($A_{z'z'}$). The values for ΔE_Q of -2.85 mm/s and δ of 0.25 mm/s (at 4.2 K) are consistent with the known low-spin ferric configu-

Table 1: Mössbauer Parameters for NH_{light}, NH_A, and NH_{dark} at 4.2 K[a]

	δ (mm/s)	ΔE_Q (mm/s)	η	A_x (MHz)	A_y (MHz)	A_z (MHz)
NH_{light} ($S = 1/2$)	0.25	−2.85	0.4	11	−5	−56
NH_A ($S = 1/2$)	0.12[b]	−3.1	0.8	20	0	−47
NH_{dark} ($S = 0$)	0.03	1.47	0	−	−	−

[a] The z'-axis of the **A** tensor of NH_{light} is tilted by ≈45° (β) relative to the z-axis of the **g** tensor, defined by $g_z = 1.97$. For NH_A, the largest component of the EFG tensor, $V_{z'z'}$, is tilted by ≈30° (β) relative to the z'-axis of the **A** tensor; we have no information about the spatial orientation of **A** and **g** for NH_A. [b] Uncertainty of δ is ±0.1 mm/s.

ration of the iron in active nitrile hydratase, but stand in contrast to values for ΔE_Q of 0.36 mm/s and δ of 0.31 mm/s reported by Honda and co-workers for this form of the enzyme (*18*).

The **g** tensor of the ferric ion in NH_{light} is quite isotropic. Therefore, the spatial correlation of the **g** and **A** tensors cannot be obtained from frozen solution Mössbauer spectra. However, because the magnetic hyperfine tensor is very anisotropic, some relevant information regarding the spatial correlation of the **A** and **g** tensors can be obtained from the EPR spectrum of Figure 2B. It can be seen that the $g_z = 1.97$ resonance of the EPR spectrum is split into a doublet by ^{57}Fe ($I = 1/2$) magnetic hyperfine interactions. The observed splitting of approximately 1.4 mT corresponds to an A value of 40 MHz; i.e., the component of **A** along the electronic z-axis is smaller than the largest principal component of the **A** tensor, $A_{z'} \approx -56$ MHz (Table 1), showing that the principal axis frames of the **A** and **g** tensors are rotated relative to each other. An **A** tensor component of ∼40 MHz along the direction of g_z indicates that the z'-axis of the **A** tensor is rotated by ∼45° relative to the direction defined by the $g_z = 1.97$ resonance. Ignoring the low symmetry indicated by the observation that the **g** and **A** tensors have different principal axis frames (i.e., assuming a symmetry not lower than rhombic), we have employed the model developed by Griffith (*21*) and its extension to Mössbauer spectroscopy by Oosterhuis and Lang (*22*) to assess the ligand field parameters of the ferric ion in NH_{light}.[3] As elaborated on elsewhere (*21*−*26*, *32*), the tetragonal and rhombic ligand field parameters Δ/λ and V/λ can be obtained from the experimental g values (λ is the spin−orbit coupling parameter, $\lambda \approx -400$ cm^{-1}). For NH_{light}, we obtain a V/Δ of ≈0.7 and a k of 1.1 for the "orbital reduction factor"; values of k above unity indicate that the assumptions of the model (namely, ignoring contributions from e_g orbitals) are not fully justified (*24*). The ^{57}Fe magnetic hyperfine tensor can be computed with the knowledge of a V/λ of −8.1 and a Δ/λ of −11.7. For this computation, two additional parameters are required: κ, a parameter characterizing the isotropic contact contribution, and the scaling factor $P = 2\beta\beta_n\langle r^{-3}\rangle N^2$, where N^2 is a covalency factor. P accounts for the radial distribution of the valence electrons of the ferric ion, and its reduction can be attributed to covalency effects (for details, see refs *22*, *26*, and *32*).

[3] For symmetries lower than rhombic, the magnetic hyperfine interactions can acquire an antisymmetric component (*22*). To our knowledge, such a component has not yet been observed experimentally, presumably because the resolution of the spectra is insufficient.

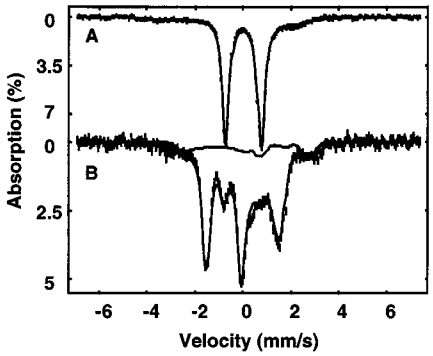

FIGURE 5: The 4.2 K Mössbauer spectra of NH_{dark} recorded in a zero magnetic field (A) and in a parallel magnetic field of 6.0 T (B). The solid line drawn through the data of spectrum B is a theoretical curve (85% of the total Fe) for NH_{dark} assuming $S = 0$, $\Delta E_Q = 1.47$ mm/s, and $\eta = 0$. The spectra also contain a fraction (15%) of NH_{light}; this contribution is outlined separately in spectrum B.

Mössbauer data for low-spin ferric heme proteins, which have been analyzed extensively with the Griffith model, have been fitted well with a κ of 0.35 and a P of ≈85 MHz (*26*, *32*). We were able to reproduce the experimental A values of NH_{light} with a κ of 0.35 and a value of P reduced to 68 MHz, yielding $A_x = 10$ MHz, $A_y = 1.3$ MHz, and $A_z = -57.6$ MHz, in good agreement with the experimental data of NH_{light} listed in Table 1.

Mössbauer Study of NH_{dark}. Figure 5 shows Mössbauer spectra of NH_{dark} recorded at 4.2 K in zero field (A) and in an applied field of 6.0 T (B). The major species of the zero-field spectrum, representing 85% of the iron, consists of a sharp doublet with a ΔE_Q of 1.47 mm/s and a δ of 0.03 mm/s. The spectrum in Figure 5B demonstrates that this doublet represents a diamagnetic site (see the figure caption), and the small value of δ is consistent with NO coordination (see below).

These data are very different from the Mössbauer spectra originally published for NH_{dark} (*18*, *27*). In that work, two components with approximately equal intensity were observed, one most likely the same as the dominant component we observe ($\Delta E_Q = 1.49$ mm/s and $\delta = 0.02$ mm/s) and one with a ΔE_Q of 0.31 mm/s and a δ of 0.31 mm/s, similar to what was seen for NH_{light} in the previous study, but unlike any component we have observed in any of our samples of the enzyme.

Irradiation of NH_{dark} at Cryogenic Temperatures. (a) Mössbauer Studies. Figure 6A shows Mössbauer spectra of a sample purified in the dark, exposed to NO on ice to reduce the fraction of NH_{light} present, and diluted 1:1 with glycerol. The only spectral component present is NH_{dark}. This sample was illuminated with white light in the Mössbauer spectrometer at 4.2 K for 1 h; after the light was turned off, the spectrum in Figure 6B was recorded for a period of 30 h. Illumination at 4.2 K resulted in the appearance of a paramagnetic component, NH_A, that accounts for 65% of the absorption (Figure 6B). The spectrum in Figure 6C was obtained by subtracting the spectrum of the dark enzyme (Figure 6A) from that shown in Figure 6B. Figure 6D compares the spectra of NH_A and NH_{light}. Although the two spectra have the same general features, the hyperfine structures of the two enzyme forms are clearly distinct.

After the spectrum in Figure 6B had been recorded, the sample temperature was increased to 70 K and kept at that

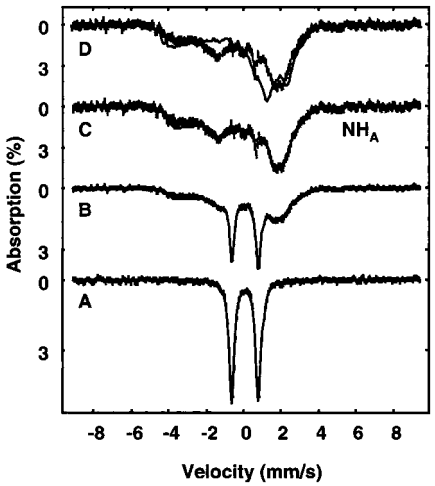

FIGURE 6: Cryogenic illumination experiments of nitrile hydratase. (A) Zero-field Mössbauer spectrum of NH_{dark}. (B) The 4.2 K spectrum recorded after illuminating NH_{dark} for 1 h at 4.2 K. (C) Spectrum of NH_A obtained by subtracting the spectrum of NH_{dark} (35%) from spectrum B. The solid line is a theoretical curve for NH_A generated from eq 1 using the parameters listed in Table 1. The solid line in spectrum B is the same theoretical spectrum plus a 35% contribution from NH_{dark}. (D) Comparison of the experimental spectra of NH_A and NH_{light} (solid line, same spectrum as in Figure 2A).

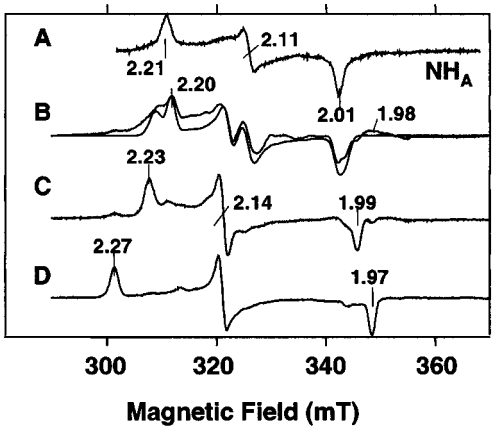

FIGURE 7: EPR spectra of nitrile hydratase following illumination at cryogenic temperatures. (A) Spectrum of NH_A (=NH_C) obtained by illuminating in the cavity of the EPR spectrometer at 20 K for 30 min with a xenon arc lamp. The spectrum was recorded at 20 K with a microwave power of 0.01 mW, a modulation amplitude of 1mT, and a frequency of 9.46 GHz; the sample did not contain glycerol. (B) Spectrum recorded at 25 K after illuminating a different sample at ≈2 K for 30 min with white light from a projector lamp. The sample contained 50% glycerol. The smooth line is a spectral simulation assuming equal contributions from two species with the following values: $g_x = 2.205$ (13.2), $g_y = 2.11$ (8.25), and $g_z = 2.008$ (7.42) and $g_x = 2.133$ $g_y = 2.225$, and $g_z = 2.00$ [line widths (gauss), in parentheses, are the same for both species]. (C) Spectrum obtained at 25 K after the temperature of the sample used to record spectrum B was raised to ≈77 K where it was kept for 1 h. (D) Spectrum of the sample used to record spectrum C after storage in liquid nitrogen for 3 days (see the text). Experimental conditions for spectra B−D: temperature, 25 K; frequency, 9.62 GHz; modulation amplitude, 0.98 mT; microwave power (B) 1, (C) 1.6, and (D) 2 mW. Spectrum A was redrawn to be correct for 9.62 GHz for purposes of comparison.

temperature for 15 min before the sample was cooled again to 4.2 K; the Mössbauer spectrum subsequently recorded was the same as that of Figure 6A.

We have also performed Mössbauer illumination studies at 150 and 180 K. After illumination of a sample of NH_{dark} for 15 min at 150 K, we recorded the spectrum of Figure 4B (hatch marks). This spectrum exhibits two quadrupole doublets, namely, a majority species (∼60%) belonging to NH_{dark} and a new doublet (species NH_B), asymmetrically broadened by relaxation, with a ΔE_Q of 2.6 mm/s and a δ of 0.23 mm/s at 150 K. The same spectrum was obtained at 180 K after further illuminating the sample at 180 K for 2 h. The observation of doublet NH_B, distinct from that of the doublet of NH_{dark}, suggests that NO escapes from the active site at >150 K. Moreover, the absence of NH_{light} from the high-temperature spectra indicates that in this experiment NH_{dark} was not transformed into NH_{light} while maintaining the protein at 180 K for ∼24 h. Because the Mössbauer spectra of NH_A (and NH_B) differ from those of NH_{light}, and because ENDOR studies of NH_{light} indicate an OH^- ligand in the sixth coordination position of the Fe^{3+} ion, our results suggest that NH_A ions (and perhaps NH_B) are low-spin, five-coordinate ferric complexes formed by photodissociation of the nitrosyl ligand at 4.2 K (note that the sample of NH_{light} studied by ENDOR spectroscopy was prepared by illumination at 4 °C prior to freezing).

(b) EPR Studies. Prior to the Mössbauer illumination studies, we had obtained EPR spectra of cryogenically irradiated NH_{dark} at DuPont. Illumination of NH_{dark} at 20 K using a xenon arc lamp resulted in a new EPR spectrum (Figure 7A) with g values at 2.21, 2.11, and 2.01. This species corresponds most likely to Mössbauer component NH_A. Warming this sample to 77 K followed by cooling to 20 K led to the disappearance of the spectrum, in agreement with the results obtained by Mössbauer spectroscopy. Double integration of the signal of Figure 7A gave ≈0.5 spin/Fe; however, spin concentrations as high as 0.9 spin/Fe were obtained by illumination at 4 K, although those samples contained additional (minor) spectral components. All of these enzyme samples were fully active after photoactivation at 4 °C.

The EPR spectrum of NH_C was also obtained when NH_{dark} was irradiated at 20 K in the presence of either butyric acid or phenylhydrazine at concentrations that would be sufficient to inhibit the enzyme at room temperature; the presence of these inhibitors of nitrile hydration does induce significant perturbation of the EPR spectrum of NH_{light} (*10*, *28*). In contrast, the presence of isobutyronitrile, another inhibitor of nitrile hydration, effectively prevented formation of NH_C. These results suggest that butyric acid and phenylhydrazine do not bind to NH_{dark} under these conditions, even though they are competitive inhibitors of NH_{light}, while isobutyronitrile does appear to bind to NH_{dark} and prevent photodissociation of NO.

On the basis of the observation that rebinding of NO occurs at 77 K for both NH_A and NH_C, we suspect that they are identical species. This species is probably a five-coordinate ferric complex formed by photolysis of the Fe−NO bond, and the reappearance of NH_{dark} after warming to 77 K indicates rebinding of NO at that temperature. Complete rebinding of NO within 15 min at 77 K would require that NO be sequestered in the vicinity of the iron site. This suggested to us that one should be able to obtain EPR evidence for the presence of an NO radical, either as an independent species or as a species interacting with the low-

spin ferric ion. EPR spectral simulations indicated that dipolar interactions between the radical and the iron should be detectable if the two species were closer than ~12 Å. However, such interactions are not apparent in the spectra; for example, see Figure 7A. It is conceivable that the photodissociated NO binds at multiple sites in a nonspecific manner, producing distributed g values that give rise to broad EPR features not readily detected at the low NO concentrations used in the experiments described here. Broad, ill-defined EPR spectra arising from distributed binding sites have been reported for nitric oxide adsorbed in zeolites (*29*). We have also considered the remote possibility that the NO signal was not detected because its spin relaxes rapidly at ~20 K. However, the EPR spectra of the Fe(III) site exhibit severe passage effects at $T < 15$ K, indicating very slow relaxation; spectra recorded down to 2.2 K did not reveal any features that could possibly be attributed to NO.

We were intrigued by the lack of EPR evidence for the NO radical that should have been produced by the photolysis, so we carried out an additional EPR illumination experiment (Figure 7B−D). It should be noted that that this sample contained 50% glycerol, as did the Mössbauer sample of Figure 6, in contrast to the sample studied at DuPont (Figure 7A) which was studied in glycerol-free buffer. By illuminating the species at ~2 K, we obtained the spectrum of Figure 7B. The major species that is observed is the same as that seen in Figure 7A. However, the sample exhibits a second species with g values at 2.22, 2.13, and 2.00. The smooth solid line drawn in Figure 7B is a spectral simulation for which we assumed that the two species are in a 1:1 concentration ratio. The spectrum also contains a feature around $g = 1.98$ that is reminiscent of dissolved NO. Moreover, there are features between $g = 2.15$ and 2.20 for which the simulation does not account. The appearance of multiple species in EPR spectra of samples irradiated at the lowest temperatures studied, ≤4 K, is consistent with previous results obtained at DuPont. However, increasing the sample temperature to 77 K, and maintaining that temperature for 60 min, led to the conversion of these signals to a new spectrum with g values at 2.23, 2.14, and 1.99 (Figure 7C, spectrum recorded at 25 K), rather than to the expected disappearance of the signals. After the spectrum of Figure 7C was recorded, the sample was removed from the EPR dewar and transferred into a liquid nitrogen dewar used for sample storage. Even though the transfer process takes less than 15 s, the sample can experience a temperature excursion up to 130 K (measured by placing a thermistor into a water-filled EPR tube). After storing the sample in the dark for 3 days under liquid nitrogen, we recorded the EPR spectrum again at 25 K. To our surprise, the iron center had converted to NH_{light} (Figure 7D). Note that the EPR spectra of Figure 7B−D each represent about 0.1 spin/Fe, indicating a much lower illumination yield than those obtained with EPR at DuPont or with Mössbauer spectroscopy.

DISCUSSION

The role of nitric oxide in the photoactivation of nitrile hydratase has been demonstrated previously (*8*) by irradiation of the inactive form, NH_{dark}, at 0 °C. The active form of the enzyme (NH_{light}) obtained in this way is characterized by an EPR signal with g values around 2.27, 2.13, and 1.97 (*10*). We have studied the Mössbauer and EPR spectra of both NH_{dark} and NH_{light} forms of nitrile hydratase, together with those of some species trapped following the illumination of the NO-bound enzyme at low temperatures.

Our Mössbauer spectra differ significantly from those reported previously by other investigators (*18*, *27*). Honda et al. associated a quadrupole doublet with a ΔE_Q of 0.36 mm/s and a δ of 0.31 mm/s with the active enzyme (Figure 2 in ref *18*). This assignment cannot be correct for the following reasons. There is general agreement that the $S = {}^1/_2$ EPR signal with g values near 2.27, 2.13, and 1.97 originates from the active form of the enzyme. Therefore, the Mössbauer spectrum associated with this form of the enzyme must exhibit paramagnetic hyperfine structure at low temperatures. The species labeled B in refs *18* and *27* exhibits a quadrupole doublet at 9 K (Figure 2 in ref *18*), rather than a magnetically split spectrum. For a sample of the inactive enzyme, which lacked an EPR signal (Figure 2 in ref *27*), these authors observed two quadrupole doublets: doublet B and a doublet with the same parameters as we report for NH_{dark}. Because the two doublets seemed to have equal intensities, Nagamune et al. proposed that nitrile hydratase contained a binuclear iron site. This hypothesis has been dispelled by subsequent crystallographic studies. While we do not have an explanation for the previously published Mössbauer results, we note that nothing in our data for NH_{dark} or NH_{light} is inconsistent with other published studies of the enzyme.

The quadrupole splitting and isomer shift of NH_{light} that we observe are typical of low-spin Fe^{3+} complexes. Fits to the Mössbauer spectra of NH_{light} with eq 1 and analysis of the parameters with the Griffith model (*22*, *23*) gave a scaling constant for the magnetic hyperfine interactions ($P = 2\beta\beta_n\langle r^{-3}\rangle N^2 = 68$ MHz) that is considerably smaller than the P of ≈85 MHz generally found for low-spin Fe^{3+} hemes, but similar to a P of 67 MHz observed for Fe(III) bleomycin (*30*). The low value obtained for P indicates significantly higher covalency for the low-spin iron of nitrile hydratase. Our studies have also shown that the ligand field of NH_{light} has lower than rhombic symmetry, as revealed by the observation that the **A** tensor is significantly rotated relative to the **g** tensor. Mössbauer spectroscopy of frozen solution samples is not well suited to determining the orientation of the **A** tensor relative to a rather *isotropic* **g** tensor, and therefore, we have combined Mössbauer spectroscopy with EPR to gain information about the spatial relation between the **g** tensor and the ^{57}Fe magnetic hyperfine tensor. However, to gain more precise data on the relative orientation of the two tensors, techniques such as ENDOR should be employed.

The metal center in NH_{dark} comprises a formal $Fe^{3+}-NO$ complex, consistent with the photodissociation of a neutral NO species to yield the low-spin ferric complex of NH_{light}. There are few characterized examples of such $\{Fe-NO\}^6$ complexes [nomenclature of Enemark and Feltham (*31*)], and those that have been studied by Mössbauer spectroscopy have parameters similar to those observed here. For instance, Wieghardt and co-workers (*32*) have reported for *trans*-$[(cyclam)Fe(NO)Cl]^{2+}$ values for δ of 0.04 mm/s, ΔE_Q of 2.05 mm/s, and η of 0 that compare very well with values for δ of 0.03 mm/s, ΔE_Q of 1.47 mm/s, and η of 0 obtained here for NH_{dark}. Given that a low-spin ferric complex results from photodissociation of the NO as a radical, one might be

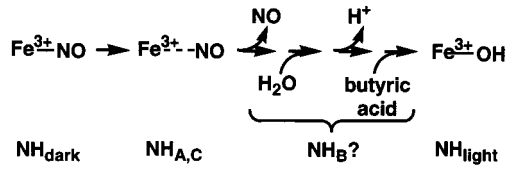

FIGURE 8: Hypothetical scheme for the photoactivation of nitrile hydratase.

inclined to consider the Fe site in NH_{dark} as low-spin Fe^{3+}. However, two observations argue against such an assignment. First, the isomer shift is quite small compared to that of normal Fe^{3+} complexes ($\delta \approx 0.15-0.35$ mm/s), and second, a low-spin Fe^{3+} in an octahedral environment has an unpaired spin in a t_{2g} orbital that would yield a negative value for ΔE_Q. By studying the isomer shifts of Fe−cyclam complexes in various oxidation states (see Figure 12 in ref *32*), Hauser et al. have concluded that $\{Fe-NO\}^6$ complexes have substantial $Fe^{4+}-NO^-$ admixture, and that the electronic structure is perhaps best described as a low-spin Fe^{4+} ($S = 1$) strongly antiferromagnetically coupled to a NO^- ($S = 1$) ligand. Our Mössbauer data suggest that this interpretation applies to NH_{dark} as well.

We have performed a series of cryogenic irradiation Mössbauer and EPR experiments. By illuminating the NO-bound form of nitrile hydratase in the Mössbauer dewar at <20 K, we have obtained a new state of the enzyme, NH_A, that differs significantly from the active enzyme, NH_{light}. It is reasonable to assume that this new species represents a five-coordinate complex resulting from the NH_{dark} form by photolysis of the $Fe^{3+}-NO$ bond. At 4.2 K, the Mössbauer data show that no significant rebinding of the dissociated NO occurs during the time required to collect the spectrum (∼30 h). In contrast, complete rebinding of NO was observed within 15 min after the temperature of the Mössbauer sample was increased to 70 K, while the sample was maintained in the dark. This suggests that NH_A is an intermediate in the photoactivation process that is trapped at 4.2 K. Photolysis performed in the Mössbauer cryostat at 150 K gave species NH_B in ∼40% yield. This species has a quadrupole splitting close to, but nevertheless different from, that observed at 150 K for NH_{light}, showing that it, too, is a distinct state of the enzyme. The extent to which the local environment of the Fe^{3+} site of NH_B differs from that observed for NH_A is not clear. However, NH_A and NH_B differ in one aspect; namely, NO rebinds readily to yield NH_{dark} when NH_A is briefly warmed to 77 K, while the NO ligand escapes when NH_{dark} is photolyzed at 150 K. NH_B may also be an intermediate in photoactivation. A hypothesis for the involvement of NH_A and NH_B in the photoactivation mechanism is shown in Figure 8.

In assessing the low-temperature photolysis results, the reader has to keep in mind that the various experiments were not performed under identical conditions. Thus, the EPR experiments that led to the spectrum of Figure 7A involved samples that lacked glycerol, while the EPR experiments that led to Figure 7B−D and all of the Mössbauer experiments involved a 50:50 (v/v) buffer/glycerol solution. It is well established that the presence of glycerol can affect protein conformation and active site structure. Moreover, the illumination conditions differed substantially in our experiments. EPR illumination of NH_{dark} between 4 and 20 K at DuPont and Mössbauer illumination at 4.2 K at Carnegie Mellon gave similar results, in both cases giving rise to new species (NH_C and NH_A, respectively) that reverted to NH_{dark} upon warming to ∼70 K. Because both species reverted to NH_{dark} when the samples were warmed, we suspect that NH_A and NH_C are the same species.

We do not fully understand the results displayed in Figure 7B−D, for a variety of reasons. First, the sample did not revert back to NH_{dark} after warming to 77 K and cooling to 25 K. Rather, the spectrum of Figure 7C was observed. It appears that subtle differences in sample preparation have provided a protein conformation that either allows NO to escape from the active site or prevents a sequestered NO from returning to the iron. Second, the protein conformation giving rise to the EPR signal of Figure 7C is capable of converting into NH_{light} at <130 K.

An obvious goal for further illumination experiments is to search for the EPR signature of the photodissociated ligand. Because rebinding occurred readily in the experiments whose results are depicted in Figures 6 and 7A, the ligand must have been sequestered in the vicinity of the active site after illumination at 20 K. Because the active site contains a low-spin ($S = {}^1/_2$) ferric ion after photolysis, the photolyzed ligand must be in the $NO^\bullet$ ($S = {}^1/_2$) form and should yield an EPR signature. EPR spectra (not shown) of saturated solutions of NO in samples of bovine serum albumin show broad features extending from $g = 2.00$ to 1.96. It is likely that such a species would be difficult to observe for the concentrations (<0.2 mM) and spectrometer conditions used for the experiment whose results are depicted in Figure 7A.

ACKNOWLEDGMENT

We thank Dr. Michael Hendrich for allowing us to use his EPR simulation programs and for useful discussions about the EPR data.

REFERENCES

1. Yamada, H., and Kobayashi, M. (1996) *Biosci., Biotechnol., Biochem. 60*, 1391−1400.
2. Nakajima, Y., Doi, T., Satoh, Y., Fujiwara, A., and Watanabe, I. (1987) *Chem. Lett.*, 1767−1770.
3. Nagamune, T., Kurata, H., Hirata, M., Honda, J., Koike, H., Ikeuchi, M., Inoue, Y., Hirata, A., and Endo, I. (1990) *Biochem. Biophys. Res. Commun. 168*, 437−442.
4. Honda, J., Kandori, H., Okada, T., Nagamune, T., Shichida, Y., Sasabe, H., and Endo, I. (1994) *Biochemistry 33*, 3577−3583.
5. Noguchi, T., Honda, J., Nagamune, T., Sasabe, H., Inoue, Y., and Endo, I. (1995) *FEBS Lett. 358*, 9−12.
6. Noguchi, T., Hoshino, M., Tsujimura, M., Odaka, M., Inoue, Y., and Endo, I. (1996) *Biochemistry 35*, 16777−16781.
7. Bonnet, D., Artaud, I., Moali, C., Petre, D., and Mansuy, D. (1997) *FEBS Lett. 409*, 216−220.
8. Odaka, M., Fujii, K., Hoshino, M., Noguchi, T., Tsujimura, M., Nagashima, S., Yohda, M., Nagamune, T., Inoue, Y., and Endo, I. (1997) *J. Am. Chem. Soc. 119*, 3785−3791.
9. Nagasawa, T., Ryuno, K., and Yamada, H. (1986) *Biochem. Biophys. Res. Commun. 139*, 1305−1312.
10. Sugiura, Y., Kuwahara, J., Nagasawa, T., and Yamada, H. (1987) *J. Am. Chem. Soc. 109*, 5848−5850.
11. Nelson, M. J., Jin, H., Turner, I. M., Jr., Grove, G., Scarrow, R. C., Brennan, B. A., and Que, J. L. (1991) *J. Am. Chem. Soc. 113*, 7072−7073.
12. Jin, H., Turner, I. M., Jr., Nelson, M. J., Gurbiel, R. J., Doan, P. E., and Hoffman, B. M. (1993) *J. Am. Chem. Soc. 115*, 5290−5291.

13. Doan, P. E., Nelson, M. J., Jin, H. Y., and Hoffmann, B. M. (1996) *J. Am. Chem. Soc. 118*, 7014−7015.
14. Brennan, B. A., Cummings, J. G., Chase, D. B., Turner, I. M., and Nelson, M. J. (1996) *Biochemistry 35*, 10068−10077.
15. Scarrow, R. C., Brennan, B. A., Cummings, J. G., Jin, H. Y., Duong, D. H. J., Kindt, J. T., and Nelson, M. J. (1996) *Biochemistry 35*, 10078−10088.
16. Huang, W. J., Jia, J., Cummings, J., Nelson, M., Schneider, G., and Lindqvist, Y. (1997) *Structure 5*, 691−699.
17. Nagashima, S., Nakasako, M., Dohmae, N., Tsujimura, M., Takio, K., Odaka, M., Yohda, M., Kamiya, N., and Endo, I. (1998) *Nat. Struct. Biol. 5*, 347−351.
18. Honda, J., Teratani, Y., Kobayashi, Y., Nagamune, T., Sasabe, H., Hirata, A., Ambe, F., and Endo, I. (1992) *FEBS Lett. 301*, 177−180.
19. Scarrow, R. C., Strickler, B. S., Ellison, J. J., Shoner, S. C., Kovacs, J. A., Cummings, J. G., and Nelson, M. J. (1998) *J. Am. Chem. Soc. 120*, 9237−9245.
20. Münck, E. (1978) *Methods Enzymol. 54*, 346−396.
21. Griffith, J. S. (1957) *Nature 180*, 30−31.
22. Oosterhuis, W. T., and Lang, G. (1969) *Phys. Rev. 178*, 439−456.
23. Sharrock, M. (1976) *Biochim. Biophys. Acta 420*, 8−26.
24. Griffith, J. S. (1971) *Mol. Phys. 21*, 135−139.
25. Abragam, A., and Bleaney, B. (1970) *Electron Paramagnetic Resonance of Transition Ions*, Clarendon Press, Oxford, U.K., Chapter 8, p 481.
26. Walker, F. A. (1999) *Coord. Chem. Rev. 185−186*, 471−534.
27. Nagamune, T., Honda, J., Kobayashi, Y., Sasabe, H., Endo, I., Ambe, F., Teratani, Y., and Hirata, A. (1992) *Hyperfine Interact. 71*, 1271−1274.
28. Sugiura, Y., Kuwahara, J., Nagasawa, T., and Yamada, H. (1988) *Biochem. Biophys. Res. Commun. 154*, 522−528.
29. Kasai, P. H., and Bishop, R. J. (1972) *J. Am. Chem. Soc. 94*, 5560−5566.
30. Burger, R. M., Kent, T. A., Horwitz, S. B., Munck, E., and Peisach, J. (1983) *J. Biol. Chem. 258*, 1559−1564.
31. Enemark, J. H., and Feltham, R. D. (1974) *Coord. Chem. Rev. 13*, 339−406.
32. Hauser, C., Glaser, T., Bill, E., Weyhermüller, T., and Wieghardt, K. (2000) *J. Am. Chem. Soc. 122*, 4352−4343.

BI010198F